



Future  
vegetation–climate  
interactions in  
Eastern Siberia

A. Arneth et al.

# Future vegetation–climate interactions in Eastern Siberia: an assessment of the competing effects of CO<sub>2</sub> and secondary organic aerosols

A. Arneth<sup>1</sup>, R. Makkonen<sup>2</sup>, S. Olin<sup>3</sup>, P. Paasonen<sup>2</sup>, T. Holst<sup>3</sup>, M. K. Kajos<sup>2</sup>, M. Kulmala<sup>2</sup>, T. Maximov<sup>4</sup>, P. A. Miller<sup>3</sup>, and G. Schurgers<sup>3,5</sup>

<sup>1</sup>Karlsruhe Institute of Technology, Institute of Meteorology and Climate Research/Atmospheric Environmental Research, Garmisch Partenkirchen, Germany

<sup>2</sup>Department of Physics, University of Helsinki, P.O. Box 64, University of Helsinki, 00014 Helsinki, Finland

<sup>3</sup>Department of Physical Geography and Ecosystem Science, Lund University, Sölvegatan 12, 22362 Lund, Sweden

<sup>4</sup>Department of Plant Ecological Physiology and Biochemistry Lab., Institute for Biological Problems of Cryolithozone SB RAS, 41, Lenin ave, 677980 Yakutsk, Russia

<sup>5</sup>Department of Geosciences and Natural Resource Management, University of Copenhagen, Øster Voldgade 10, 1350 Copenhagen, Denmark

Title Page

Abstract

Introduction

Conclusions

References

Tables

Figures



Back

Close

Full Screen / Esc

Printer-friendly Version

Interactive Discussion



Received: 21 August 2015 – Accepted: 22 September 2015 – Published: 7 October 2015

Correspondence to: A. Arneth (almut.arneth@kit.edu)

Published by Copernicus Publications on behalf of the European Geosciences Union.

**ACPD**

15, 27137–27175, 2015

**Future  
vegetation–climate  
interactions in  
Eastern Siberia**

A. Arneth et al.

Title Page

Abstract

Introduction

Conclusions

References

Tables

Figures



Back

Close

Full Screen / Esc

Printer-friendly Version

Interactive Discussion



## Abstract

Disproportional warming in the northern high latitudes, and large carbon stocks in boreal and (sub)arctic ecosystems have raised concerns as to whether substantial positive climate feedbacks from biogeochemical process responses should be expected. Such feedbacks occur if increasing temperatures lead to e.g. a net release of CO<sub>2</sub> or CH<sub>4</sub>. However, temperature-enhanced emissions of biogenic volatile organic compounds (BVOC) have been shown to contribute to the growth of secondary organic aerosol (SOA) which is known to have a negative radiative climate effect. Combining measurements in Eastern Siberia with model-based estimates of vegetation and permafrost dynamics, BVOC emissions and aerosol growth, we assess here possible future changes in ecosystem CO<sub>2</sub> balance and BVOC-SOA interactions, and discuss these changes in terms of possible climate effects. On global level, both are very small but when concentrating on Siberia and the northern hemisphere the negative forcing from changed aerosol direct and indirect effects become notable – even though the associated temperature response would not necessarily follow a similar spatial pattern. While our analysis does not include other important processes that are of relevance for the climate system, the CO<sub>2</sub> and BVOC-SOA interplay used serves as an example of the complexity of the interactions between emissions and vegetation dynamics that underlie individual terrestrial feedbacks and highlights the importance of addressing ecosystem-climate feedbacks in consistent, process-based model frameworks.

## 1 Introduction

Warming effects on ecosystem carbon cycling in northern ecosystems (Serreze et al., 2000; Tarnocai et al., 2009), and the potential for large climate-feedbacks from losses of CO<sub>2</sub> or CH<sub>4</sub> from these carbon-dense systems have been widely discussed (Khvorostyanov et al., 2008; Schuur et al., 2009; Arneth et al., 2010). Other biogeochemical processes can also lead to feedbacks, in particular through emissions of

### Future vegetation–climate interactions in Eastern Siberia

A. Arneth et al.

Title Page

Abstract

Introduction

Conclusions

References

Tables

Figures



Back

Close

Full Screen / Esc

Printer-friendly Version

Interactive Discussion









## Future vegetation–climate interactions in Eastern Siberia

A. Arneth et al.

Title Page

Abstract

Introduction

Conclusions

References

Tables

Figures

◀

▶

◀

▶

Back

Close

Full Screen / Esc

Printer-friendly Version

Interactive Discussion



across the size range of 6–600 nm were completed every 5 min. The SMPS data were used to determine occasions of aerosol particle nucleation. The growth rates were calculated from log-normal modes fitted to the measured particle size distribution following Hussein et al. (2005). The time evolution of the diameters at which the fitted modes peaked was inspected visually, and the growth rate was determined with linear least squares fitting to these peak diameters whenever a continuous increase in diameter was observed. In this analysis we calculated growth rates for particles from 25 to 160 nm.

The source rate for condensing vapour ( $Q$ ) was determined by calculating the concentration of condensable vapour needed to produce the observed growth rate ( $C_{GR}$ , Nieminen et al., 2010) and the condensation sink from the particle size distribution (CS, Kulmala et al., 2001). In steady state the sources and sinks for the condensing vapour are equal, and thus we determined the source rate as  $Q = C_{GR} \cdot CS$ .

## 2.2 Modelling of dynamic vegetation processes, permafrost and BVOC emissions

We applied the dynamic global vegetation model LPJ-GUESS (Smith et al., 2001; Sitch et al., 2003), including algorithms to compute canopy BVOC emission following Niinemets et al. (1999), Arneth et al. (2007b) and Schurgers et al. (2009a), and permafrost as adopted from Wania et al. (2009). LPJ-GUESS simulates global and regional dynamics and composition of vegetation in response to changes in climate and atmospheric  $CO_2$  concentration. Physiological processes like photosynthesis, autotrophic and heterotrophic respiration are calculated explicitly, a set of carbon allocation rules determines plant growth. Plant establishment, growth, mortality, and decomposition, and their response to resource availability (light, water) modulate seasonal and successional population dynamics arising from a carbon allocation trade-off (Smith et al., 2001). Fire disturbance is included in the model (Thonicke et al., 2001). Similar to other DGVMs, a number of plant functional types (PFT) are specified to represent the larger global vegetation units (Sitch et al., 2003). Model results compare well with

## Future vegetation–climate interactions in Eastern Siberia

A. Arneth et al.

Title Page

Abstract

Introduction

Conclusions

References

Tables

Figures



Back

Close

Full Screen / Esc

Printer-friendly Version

Interactive Discussion



observations on LAI, permafrost distribution and vegetation response to warming (see results). Total present-day modelled soil C pools over the top 2 m in Eastern Siberia are 216 Gt C, and 454 Gt C for circumpolar soils above 40° N (Table 1). A recent data-base estimate was 191, 495, and 1024 Gt C in the 0–30, 0–100 and 0–300 cm soil layer, of permafrost-affected soils, respectively (Tarnocai et al., 2009). These numbers indicate that the values calculated with LPJ-GUESS are lower than observation-based ones, most likely underestimating C-density in particular in the soil layers below few tenths of cm.

BVOC emissions models, whether these are linked to DGVMs or to a prescribed vegetation map, all rely on using emission potentials ( $E^*$ , leaf emissions at standardised environmental conditions) or some derivatives in their algorithms. In LPJ-GUESS, production and emissions of leaf and canopy isoprene and monoterpenes are linked to their photosynthetic production, specifically the electron transport rate, and the requirements for energy and redox-equivalents to produce a unit of isoprene from triose-phosphates (Niinemets et al., 1999; Arneth et al., 2007b; Schurgers et al., 2009a). A specified fraction of absorbed electrons used for isoprene (monoterpene) production ( $\varepsilon$ ) provides the link to PFT-specific  $E^*$  (Arneth et al., 2007a); in case of monoterpenes emitted from storage an additional correction is applied to account for their light-dependent production (taking place over parts of the day) and temperature-driven (taking place the entire day) emissions (Schurgers et al., 2009a).

Leaf BVOC emissions are stimulated in a future environment in response to warmer temperatures. Moreover, warmer temperatures and CO<sub>2</sub>-fertilisation of photosynthesis lead to enhanced vegetation productivity and leaf area, with additional positive effects on BVOC emissions. But higher CO<sub>2</sub> concentrations have also been shown to inhibit leaf isoprene production. Even though the underlying metabolic mechanism is not yet fully understood, this effect has been observed in a number of studies (for an overview see Fig. 6 in Arneth et al., 2011). Due to limited experimental evidence, whether or not a similar response occurs in monoterpene producing species cannot yet be confirmed, especially in species that emit from storage. The model is set-up to test this





green (BNS) PFT, and for other PFTs the global parameterisation was used (Schurgers et al., 2009a).

LPJ-GUESS was recently expanded with a permafrost module following Wania et al. (2009) and Miller and Smith (2012) in which a numerical solution of the heat diffusion equation was introduced. The soil column in LPJ-GUESS now consists of a snow layer of variable thickness, a litter layer of fixed thickness (5 cm), and a soil column of depth 2 m (with sublayers of thickness 0.1 m) from which plants can extract non-frozen water above the wilting point. A “padding” column of depth 48 m (with thicker sublayers) is also present beneath these three layers to aid in the accurate simulation of temperatures in the overlying compartments (Wania et al., 2009). Soil temperatures throughout the soil column are calculated daily, and change in response to changing surface air temperature and precipitation input, as well as the insulating effects of the snow layer and phase changes in the soil’s water.

Here we run the model with 0.5° spatial resolution, using climate and atmospheric CO<sub>2</sub> as driving variables as described in the literature (Smith et al., 2001). Values for the BNS “larch” PFT were adopted from previous studies (Sitch et al., 2003; Hickler et al., 2012; Miller and Smith, 2012), but with the degree-day cumulative temperature requirements on a five-degree basis (GDD5) to attain full leaf cover reduced from 200 to 100 (Moser et al., 2012). Minimum GDD5 to allow establishment was set to 350 resulting in establishment of seedlings in very cold locations. Soil thermal conductivity was  $2 \text{ W m}^{-1} \text{ K}^{-1}$ . The modelled distribution of larch in LPJ-GUESS (Fig. 1) compares well with observation-based maps (Wagner, 1997). The model was spun up for 500 years to 1900 values using CO<sub>2</sub> concentration from the year 1900 and repeating de-trended climate from 1901–1930 from CRU (Mitchell and Jones, 2005). Historical (20th century) simulations used observed CO<sub>2</sub> concentrations and were based on variable CRU climate. Simulations for the 21st century were based on ECHAM climate, using RCP8.5 emissions (Riahi et al., 2007). The model requires daily radiation, precipitation and maximum and minimum air temperatures as input (Arneth et al., 2007b). The generated GCM climate was interpolated to the CRU half-degree grid, and monthly

**Future  
vegetation–climate  
interactions in  
Eastern Siberia**

A. Arneth et al.

Title Page

Abstract Introduction

Conclusions References

Tables Figures

◀ ▶

◀ ▶

Back Close

Full Screen / Esc

Printer-friendly Version

Interactive Discussion





---

## Future vegetation–climate interactions in Eastern Siberia

A. Arneth et al.

---

[Title Page](#)[Abstract](#)[Introduction](#)[Conclusions](#)[References](#)[Tables](#)[Figures](#)[Back](#)[Close](#)[Full Screen / Esc](#)[Printer-friendly Version](#)[Interactive Discussion](#)

Whether or not BVOCs can increase the availability of cloud condensation nuclei (CCN) depends on the availability of sub-CCN sized particles (O'Donnell et al., 2011). Anthropogenic primary emissions are introduced to the model as 60 nm particles, hence condensation of sulfuric acid and organic vapours is generally needed in order to grow these particles to CCN sizes. In Siberia, the modelled primary particle emissions are dominated by wildfires, which are assumed to inject large particles with 150 nm diameter. The model is using T63 spectral resolution with 31 vertical hybrid sigma levels.

ECHAM5.5-HAM2 was run with different BVOC emission scenarios in year 2000 and 2100 simulated offline with LPJ-GUESS (see previous section). The simulations apply present-day oxidant fields as in Stier et al. (2005). The assumption of unchanging oxidant fields induces some uncertainty for future simulations and inconsistency with present-day simulations with varying biogenic emissions, since both anthropogenic and biogenic emissions are likely to modify the atmospheric oxidative capacity. All simulations are initiated with a six months spin-up, followed by 5 years of simulation for analysis. The model climate is nudged towards ERA-40 reanalysis year 2000 meteorology, an approach that is widely used in aerosol-climate assessments (K. Zhang et al., 2014). Nudging towards reanalysis meteorology establishes evaluation of BVOC-aerosol coupling with unchanged meteorological fields, but restricts the model in terms of aerosol-climate feedbacks, since e.g. nudging future climate simulations with present-day meteorological winds is based on the assumption that e.g. cloudiness, or wind direction and – speed etc. are not changing. Present-day wildfire and anthropogenic aerosol and precursor emissions are applied for all simulations (Dentener et al., 2006). One of the foci here are BVOC, comparing present-day and future BVOC emissions with  $E^* = 1.9 \mu\text{g C m}^{-2} (\text{leaf}) \text{h}^{-1}$ , but keeping other emissions constant. The emissions of dust and sea salt are modelled interactively (Zhang et al., 2012).

The analysis of model results includes total particle number concentration (CN) and cloud condensation nuclei at 1 % supersaturation (CCN (1 %)). The simulations are also used to assess the radiative effects of SOA. In the simulations, the aerosol con-

centrations are interactively coupled to the cloud-microphysics scheme (Lohmann et al., 2007) and to the direct aerosol radiative calculation. The aerosol indirect effect is evaluated as a change in cloud radiative forcing ( $\Delta\text{CRF}$ ). The direct aerosol effect accounts only for clear-sky short-wave forcing ( $\Delta\text{CSDRF}$ ). The radiative effects are calculated as differences from two time-averaged 5-year simulations as

$$\Delta\text{CRF} = \text{CRF}(\text{BVOC}_{2100}) - \text{CRF}(\text{BVOC}_{2000})$$

$$\Delta\text{CSDRF} = \text{CSDRF}(\text{BVOC}_{2100}) - \text{CSDRF}(\text{BVOC}_{2000}).$$

### 3 Results

#### 3.1 Present-day BVOC emissions

The dynamic global vegetation model LPJ-GUESS reproduces the present-day circumpolar permafrost distribution (Fig. 1; shown as circumpolar map for comparison with Tarnocai et al., 2009) and, with the exception of the Kamchatka peninsula, simulates also the expanse of the larch-dominated forests in Eastern Siberia (Fig. 1; Miller and Smith, 2012; Wagner, 1997). Maximum leaf area index (LAI) calculated by the model for the Spasskaya Pad forest ( $62^{\circ}15'18.4''$  N,  $129^{\circ}37'07.9''$  E, 220 m a.s.l), where the BVOC measurements were obtained, was 2.0 (averaged over years 1981–2000; not shown), and is in good agreement with the measured values during that period (1.6; Takeshi et al., 2008). For the “larch” plant functional type in LPJ-GUESS (Schurgers et al., 2009a), an emission potential of  $E^* = 2.4 \mu\text{g C m}^{-2} (\text{leaf}) \text{h}^{-1}$  was adopted in previous simulations from Guenther et al. (1995), a recommendation that at that time did not include observations from any larch species.

Kajos et al. (2013) measured for the first time MT  $E^*$  from *L. cajanderii*. Their measurements, taken over an entire growing season at Spasskaya Pad, suggested values of  $E^*$  ranging from  $1.9 \mu\text{g C m}^{-2} (\text{leaf}) \text{h}^{-1}$  at the lower end, to  $9.6 \mu\text{g C m}^{-2} (\text{leaf}) \text{h}^{-1}$  at the upper. Applying a weighted measured-average  $E^*$  of  $6.2 \mu\text{g C m}^{-2} (\text{leaf}) \text{h}^{-1}$ , in-

Title Page

Abstract

Introduction

Conclusions

References

Tables

Figures



Back

Close

Full Screen / Esc

Printer-friendly Version

Interactive Discussion



---

## Future vegetation–climate interactions in Eastern Siberia

A. Arneth et al.

---

Title Page

Abstract

Introduction

Conclusions

References

Tables

Figures



Back

Close

Full Screen / Esc

Printer-friendly Version

Interactive Discussion



creased simulated total present-day MT emissions across the Siberian larch biome from  $0.11 \text{ Tg Ca}^{-1}$  (as in Schurgers et al., 2009a) to  $0.21 \text{ Tg Ca}^{-1}$ , or to  $0.42 \text{ Tg Ca}^{-1}$  when the maximum  $E^*$  was used (Table 1). The observed range in  $E^*$ , and the calculated range in total emissions across Siberia, might reflect variability in tree microclimate or genetic variability, or was induced by (undetected) mechanic or biotic stress during the time of measurements (Staudt et al., 2001; Bäck et al., 2012; Kajos et al., 2013). While our data are insufficient to make a finite suggestion of *L. cajanderi*  $E^*$ , the measurements provide evidence for potentially substantially higher MT emissions from Siberian larch than previous estimates.

### 3.2 Present-day aerosols, and links to BVOC

New particle formation events (Fig. 2a) were observed regularly. The calculated volumetric source rates of condensing vapours ( $Q$ ), the product of vapour concentration required for the observed particle growth rate and particle loss rate (Kulmala et al., 2005), increased exponentially with temperature (Fig. 2b). MT concentrations increased with temperature as well, with a slope relatively similar to that found for the  $Q$  vs.  $T$  relationship (Fig. 2c). Consequently, a positive relationship emerged between  $Q$  and MT concentration (Fig. 2d), which supports previous field and laboratory evidence that MT and their oxidation products are a main precursor to the observed particle formation and growth.

Figure 2d shows the connection between the BVOC concentration and the formation rate of vapours causing the growth of the aerosol particles. Even though the monoterpene concentrations were measured above and the aerosol growth rates below the canopy, the observed correlation indicates that BVOC concentration is an important contributor to the regional aerosol growth and supports the theory that the condensation of organic vapour is largely responsible for the formation of secondary organic aerosol (Hallquist et al., 2009; Carslaw et al., 2010). Substantial within-canopy chemical reactions would be expected to worsen the relationship. The correlation depicted in Fig. 2d is determined in particular by the the formation of secondary organic aerosol

## Future vegetation–climate interactions in Eastern Siberia

A. Arneth et al.

Title Page

Abstract

Introduction

Conclusions

References

Tables

Figures

◀

▶

◀

▶

Back

Close

Full Screen / Esc

Printer-friendly Version

Interactive Discussion



on pre-existing aerosol particles, whereas the nucleation rate of new aerosol particles seems not to be dominated by the landscape-scale emissions and surface concentrations of BVOCs. For instance, most nucleation events in a Scots pine dominated landscape in Finland have been found in spring, when measured monoterpene concentrations in the near-surface were about one tenth of the summer time maximum (~ 60 ppt, vs. up to 500 ppt; Haapanala et al., 2007; Lappalainen et al., 2009). We found here MT concentrations of similar magnitude to these.

By contrast to temperature and BVOC concentrations, levels of radiation, which can be considered a surrogate for the concentration of the OH radical (OH<sup>•</sup>), did not affect  $Q$  (Fig. 2b), even though OH<sup>•</sup> has been considered an important player for aerosol formation. Rohrer and Berresheim (2006) showed a strong correlation between solar ultraviolet radiation and OH<sup>•</sup> concentration at the Hohenpeissenberg site in Germany. Furthermore, Hens et al. (2014) demonstrated that the day-time OH<sup>•</sup> concentrations in (especially) boreal forest depend on solar radiation. Hence, the poor relation between the source rate of condensing vapour and levels of radiation (Fig. 2b) indicates that OH-radical concentration did not have a major impact on  $Q$ . This agrees with the findings by Ehn et al. (2014) that ozone instead of OH<sup>•</sup> is an important, if not the main, atmospheric agent oxidising organic vapours into a chemical form that condenses on particle surfaces. Thus, our results indicate that factors and processes besides the concentrations of SO<sub>2</sub> and OH<sup>•</sup> seem to limit aerosol production in non-polluted environments (Kulmala et al., 2005).

### 3.3 Future carbon pools, vegetation distribution and BVOC emissions in Siberia

In a warmer environment with higher atmospheric CO<sub>2</sub> levels, the simulations indicated drastically reduced area of permafrost in Siberia (Fig. 1). Total net primary productivity in the simulated domain increased from an annual average of 3.5 to 5.9 Pg C a<sup>-1</sup> at the end of the 21st century. An overall C loss of 100 Pg C assumed to be in the form of CO<sub>2</sub> (since the model does not yet include a dynamic surface hydrology which would

## Future vegetation–climate interactions in Eastern Siberia

A. Arneth et al.

Title Page

Abstract

Introduction

Conclusions

References

Tables

Figures

◀

▶

◀

▶

Back

Close

Full Screen / Esc

Printer-friendly Version

Interactive Discussion



be necessary to assess changing methane emissions) at the end of the 21st century was calculated from the shrinking Siberian areas of permafrost (Table 1). However, warming and higher levels of atmospheric CO<sub>2</sub> led also to increasing LAI, and to larch-dominated areas showing the expected north- and north-eastwards shift (Fig. 1) compared to present-day climate (Miller and Smith, 2012). The carbon uptake in expanding vegetation into permafrost-free areas, combined with enhanced productivity across the simulation domain overcompensates for the losses from C-pools in permafrost areas (Table 1).

Future MT emissions were enhanced directly as a result of warmer leaves, and augmented by the future higher LAI of larch and evergreen conifers (Figs. 1d and A1; Table 1). Since the emissions scale with the emission factors applied, the proportional increase between present-day and future climate conditions is independent of the value of  $E^*$ . Whether or not leaf MT emissions are inhibited by increasing atmospheric CO<sub>2</sub> levels to similar degree to what was found for isoprene is difficult to assess from today's limited number of studies (e.g. Niinemets et al. (2010) and references therein). Similarities in the leaf metabolic pathways of isoprene and MT production suggest such an inhibition, but possibly this effect does not become apparent in plant species where produced MT are stored, unless the storage pools become measurably depleted by the reduced production. By contrast, species emitting MT in an “isoprene-like” fashion immediately after production should more directly reflect CO<sub>2</sub> inhibition. Evergreen conifers typically emit most MT from storage pools, although recent experiments have shown that some light-dependent emissions also contribute to total emission fluxes. Accordingly, based on the leaf-level measurements, larch could follow a hybrid pattern between emission after production and from storage (Kajos et al., 2013). Without accounting for CO<sub>2</sub> inhibition, MT emissions across the model domain more than doubled (Fig. 1; Table 1) by 2100, as a consequence of higher emissions per leaf area due to warmer temperatures, and of the larger emitting leaf area in response to higher photosynthesis.



## 4 Discussion

Boreal vegetation has been shown to respond to the recent decades' warming and increasing atmospheric CO<sub>2</sub> levels with a prolonged growing season and higher maximum LAI, similar to patterns in our simulations (Piao et al., 2006). The calculated enhanced biomass growth is in-line with experimental evidence of higher C in plant biomass in warming plots at tundra field sites (Elmendorf et al., 2012; Sistla et al., 2013). In Siberian mountain regions, an upward movement of vegetation zones has been recorded already (Soja et al., 2007), while the analysis of evergreen coniferous undergrowth abundance and age shows spread of evergreen species, especially *Pinus siberia*, into Siberian larch forest (Kharuk et al., 2007). These observations thus support the modelled shift in vegetation zones, and change in vegetation type composition and productivity. Likewise, other models with dynamic vegetation also have shown a strong expansion of broadleaved forests at the southern edge of the Siberian region in response to warming (Shuman et al., 2015).

Warming and thawing of permafrost soils is being observed at global monitoring network sites, including in Russia (Romanovsky et al., 2010). Estimates of carbon losses from northern wetland and permafrost soils in response to 21st century warming range from a few tens to a few hundreds Pg C, depending on whether processes linked to microbial heat production, thermokarst formation and surface hydrology, winter snow cover insulation, dynamic vegetation, C–N interactions, or fire are considered (Khvorostyanov et al., 2008; Schuur et al., 2009; Arneth et al., 2010; Koven et al., 2011; Schneider von Deimling et al., 2012). For instance, a modelled range of 0.07–0.23 W m<sup>-2</sup> forcing associated with a 33–114 Pg CO<sub>2</sub>-C loss from permafrost regions was found for a simulation study that was based on the RCP8.5 climate and CO<sub>2</sub> scenarios, but excluding full treatment of vegetation dynamics (Schneider von Deimling et al., 2012). In a recent literature review, Schaefer et al. (2014) found a range from cumulative 46 to 435 CO<sub>2</sub>-equivalents (accounting for CO<sub>2</sub> and CH<sub>4</sub>), or 120 ± 85 Gt C by 2100 in response to different future warming scenarios and modelling approaches. In

### Future vegetation–climate interactions in Eastern Siberia

A. Arneth et al.

Title Page

Abstract

Introduction

Conclusions

References

Tables

Figures



Back

Close

Full Screen / Esc

Printer-friendly Version

Interactive Discussion







## Future vegetation–climate interactions in Eastern Siberia

A. Arneth et al.

Title Page

Abstract

Introduction

Conclusions

References

Tables

Figures



Back

Close

Full Screen / Esc

Printer-friendly Version

Interactive Discussion



applied future scenarios, Siberian wildfire intensity was assumed to increase (Makko-  
nen et al., 2012a). When separated for areas of low and high wildfire emissions (Fig. 4)  
it becomes clear that in areas of low wildfire activity, the increase in SOA formation was  
proportionally high (60 %) in nucleation mode ( $d_p < 10$  nm), and the relative increases  
in SOA formation in Aitken, accumulation and coarse modes were 50, 31 and 40 %,  
respectively. However, the distribution of BVOC oxidation products was rather different  
in areas of high wildfire activity. SOA formation in coarse mode was more than doubled,  
while SOA in nucleation mode decreased by 30 %. It is clear that the effect of increased  
BVOC emission on particle population has distinct effects depending on existing back-  
ground aerosol distribution. Averaged over Siberian areas of low wildfire activity, the  
median (mean) increase of CCN (0.2 %) was calculated to be 1 % (7 %) due to BVOC  
emissions changes from year 2000 to year 2100, while areas of high wildfire emission  
lead to median (mean) increase of 0.3 % (0.5 %).

Even though the Siberian MT emissions more than double until 2100 (Table 1), the  
increasing wildfire emissions and decreasing new particle formation due to reductions  
in anthropogenic  $\text{SO}_2$  largely offset the effect of increased BVOC emissions on CCN  
concentration. In wildfire plumes, the simulated CCN concentrations were high even  
without BVOC-induced growth of smaller particles. The radiative effect due to BVOC  
emission change between years 2000 and 2100 was estimated from ECHAM-HAM  
simulations averaged over 5 years. The increase in BVOC emission leading to ad-  
ditional secondary organic aerosol induces a  $-0.2 \text{ W m}^{-2}$  change in direct clear-sky  
aerosol forcing over the Siberian domain until the year 2100. Furthermore, the in-  
crease in CCN concentrations leads to a strengthening of the cloud radiative effect  
by  $-0.5 \text{ W m}^{-2}$  (Table 2). These changes in radiative fluxes only take into account  
the changing BVOC emission, and the potential concurrent changes in anthropogenic  
and wildfire emissions might decrease the simulated radiative effect of biogenic SOA  
(Carslaw et al., 2013).

## 5 Implications, limitations and future progress

Up to now, studies that investigate the role of terrestrial vegetation dynamics and carbon cycle in the climate system typically account solely for CO<sub>2</sub>, while studies that look at BVOC-climate interactions often ignore other processes, especially interactions with vegetation dynamics or the CO<sub>2</sub>-balance of ecosystems. However, for understanding the full range of interactions between atmospheric composition, climate change and terrestrial processes we need a much more integrative perspective. Our analysis seeks to provide an example of how to quantify a number of climatically relevant ecosystem processes in the large Eastern Siberian region in a consistent observational and modelling framework that accounts for the multiple interactions between emissions, vegetation and soils. It poses a challenge to combine effects of well mixed greenhouse gases and locally constrained, short-lived substances. On global-scale level, the opposing estimates in radiative effects from ecosystem-CO<sub>2</sub> and BVOC-SOA interactions are miniscule but it is to be expected that some of the forcing effects from SOA could lead to a notable change in regional temperatures. Clearly, our numbers are uncertain but they pinpoint the necessity for assessing surface-atmosphere exchange processes comprehensively in climate feedback analyses. While doing so, we are aware of the fact that a number of additional processes are not included in our analysis. For instance, it remains to be investigated whether a similar picture would emerge when additional feedback mechanisms are taken into consideration, e.g. SOA formation from isoprene (Henze and Seinfeld, 2006) or effects of atmospheric water vapour on reaction rates and aerosol loads, or that some of the SOA might like to partition more to the gas-phase in a warmer climate. Likewise, neither the albedo effect of northwards migrating vegetation (Betts, 2000; W. Zhang et al., 2014), changes in the hydrology (which affects CH<sub>4</sub> and N<sub>2</sub>O vs. CO<sub>2</sub> fluxes), nor changes in C-N interactions (Zaehle et al., 2010) are considered here, which would require a coupled ESM that combines a broad range of dynamically varying ecosystem processes with full treatment of air chemistry and aerosol interactions. Quantifying the full range of terrestrial climate feedbacks, either

### Future vegetation-climate interactions in Eastern Siberia

A. Arneth et al.

Title Page

Abstract

Introduction

Conclusions

References

Tables

Figures

◀

▶

◀

▶

Back

Close

Full Screen / Esc

Printer-friendly Version

Interactive Discussion



globally or regionally, with consistent model frameworks that account for the manifold interactions is not yet possible with today's modelling tools.

*Acknowledgements.* A. Arneth acknowledges support from Swedish Research Council VR, and the Helmholtz Association ATMO Programme, and its Initiative and Networking Fund. The study was also supported by the Finnish Academy, grant 132100. The EU FP7 Bacchus project (grant agreement 603445) is acknowledged for financial support. P. A. Miller acknowledges support from the VR Linnaeus Centre of Excellence LUCCL, R. M. Makkonen acknowledges support from the Nordic Centre of Excellence CRAICC. This study is a contribution to the Strategic Research Area MERGE.

The article processing charges for this open-access publication were covered by a Research Centre of the Helmholtz Association.

## References

- Ahlström, A., Schurgers, G., Arneth, A., and Smith, B.: Robustness and uncertainty in terrestrial ecosystem carbon response to cmip5 climate change projections, *Environ. Res. Lett.*, 7, 044008, doi:10.1088/1748-9326/7/4/044008, 2012.
- Arneth, A., Miller, P. A., Scholze, M., Hickler, T., Schurgers, G., Smith, B., and Prentice, I. C.: CO<sub>2</sub> inhibition of global terrestrial isoprene emissions: Potential implications for atmospheric chemistry, *Geophys. Res. Lett.*, 34, L18813, doi:10.1029/2007GL030615, 2007a.
- Arneth, A., Niinemets, Ü., Pressley, S., Bäck, J., Hari, P., Karl, T., Noe, S., Prentice, I. C., Serça, D., Hickler, T., Wolf, A., and Smith, B.: Process-based estimates of terrestrial ecosystem isoprene emissions: incorporating the effects of a direct CO<sub>2</sub>-isoprene interaction, *Atmos. Chem. Phys.*, 7, 31–53, doi:10.5194/acp-7-31-2007, 2007b.
- Arneth, A., Schurgers, G., Hickler, T., and Miller, P. A.: Effects of species composition, land surface cover, CO<sub>2</sub> concentration and climate on isoprene emissions from European forests, *Plant Biol.*, 10, 150–162, doi:10.1055/s-2007-965247, 2008.
- Arneth, A., Harrison, S. P., Zaehle, S., Tsigaridis, K., Menon, S., Bartlein, P. J., Feichter, J., Korhola, A., Kulmala, M., O'Donnell, D., Schurgers, G., Sorvari, S., and Vesala, T.: Terrestrial biogeochemical feedbacks in the climate system, *Nat. Geosci.*, 3, 525–532, doi:10.1038/ngeo1905, 2010.

## Future vegetation–climate interactions in Eastern Siberia

A. Arneth et al.

Title Page

Abstract

Introduction

Conclusions

References

Tables

Figures



Back

Close

Full Screen / Esc

Printer-friendly Version

Interactive Discussion



## Future vegetation–climate interactions in Eastern Siberia

A. Arneth et al.

Title Page

Abstract

Introduction

Conclusions

References

Tables

Figures

◀

▶

◀

▶

Back

Close

Full Screen / Esc

Printer-friendly Version

Interactive Discussion



- Arneth, A., Schurgers, G., Lathiere, J., Duhl, T., Beerling, D. J., Hewitt, C. N., Martin, M., and Guenther, A.: Global terrestrial isoprene emission models: sensitivity to variability in climate and vegetation, *Atmos. Chem. Phys.*, 11, 8037–8052, doi:10.5194/acp-11-8037-2011, 2011.
- 5 Arneth, A., Mercado, L., Kattge, J., and Booth, B. B. B.: Future challenges of representing land-processes in studies on land-atmosphere interactions, *Biogeosciences*, 9, 3587–3599, doi:10.5194/bg-9-3587-2012, 2012.
- Bäck, J., Aalto, J., Henriksson, M., Hakola, H., He, Q., and Boy, M.: Chemodiversity of a scots pine stand and implications for terpene air concentrations, *Biogeosciences*, 9, 689–702, doi:10.5194/bg-9-689-2012, 2012.
- 10 Betts, R. A.: Offset of the potential carbon sink from boreal forestation by decreases in surface albedo, *Nature*, 408, 187–190, 2000.
- Carlsaw, K. S., Boucher, O., Spracklen, D. V., Mann, G. W., Rae, J. G. L., Woodward, S., and Kulmala, M.: A review of natural aerosol interactions and feedbacks within the Earth system, *Atmos. Chem. Phys.*, 10, 1701–1737, doi:10.5194/acp-10-1701-2010, 2010.
- 15 Carlsaw, K. S., Lee, L. A., Reddington, C. L., Pringle, K. J., Rap, A., Forster, P. M., Mann, G. W., Spracklen, D. V., Woodhouse, M. T., Regayre, L. A., and Pierce, J. R.: Large contribution of natural aerosols to uncertainty in indirect forcing, *Nature*, 503, 67–71, doi:10.1038/nature12674, 2013.
- Dentener, F., Kinne, S., Bond, T., Boucher, O., Cofala, J., Generoso, S., Ginoux, P., Gong, S., Hoelzemann, J. J., Ito, A., Marelli, L., Penner, J. E., Putaud, J.-P., Textor, C., Schulz, M., van der Werf, G. R., and Wilson, J.: Emissions of primary aerosol and precursor gases in the years 2000 and 1750 prescribed data-sets for AeroCom, *Atmos. Chem. Phys.*, 6, 4321–4344, doi:10.5194/acp-6-4321-2006, 2006.
- 20 Dolman, A. J., Maximov, T. C., Moors, E. J., Maximov, A. P., Elbers, J. A., Kononov, A. V., Waterloo, M. J., and van der Molen, M. K.: Net ecosystem exchange of carbon dioxide and water of far eastern Siberian Larch (*Larix cajanderii*) on permafrost, *Biogeosciences*, 1, 133–146, doi:10.5194/bg-1-133-2004, 2004.
- Ehn, M., Thornton, J. A., Kleist, E., Sipila, M., Junninen, H., Pullinen, I., Springer, M., Rubach, F., Tillmann, R., Lee, B., Lopez-Hilfiker, F., Andres, S., Acir, I. H., Rissanen, M., Jokinen, T., Schobesberger, S., Kangasluoma, J., Kontkanen, J., Nieminen, T., Kurten, T., Nielsen, L. B., Jorgensen, S., Kjaergaard, H. G., Canagaratna, M., Dal Maso, M., Berndt, T., Petaja, T., Wahner, A., Kerminen, V. M., Kulmala, M., Worsnop, D. R., Wildt, J., and Mentel,
- 30

## Future vegetation–climate interactions in Eastern Siberia

A. Arneth et al.

[Title Page](#)
[Abstract](#)
[Introduction](#)
[Conclusions](#)
[References](#)
[Tables](#)
[Figures](#)

[Back](#)
[Close](#)
[Full Screen / Esc](#)
[Printer-friendly Version](#)
[Interactive Discussion](#)


T. F.: A large source of low-volatility secondary organic aerosol, *Nature*, 506, 476–479, doi:10.1038/nature13032, 2014.

Elmendorf, S. C., Henry, G. H. R., Hollister, R. D., Bjork, R. G., Boulanger-Lapointe, N., Cooper, E. J., Cornelissen, J. H. C., Day, T. A., Dorrepaal, E., Elumeeva, T. G., Gill, M., Gould, W. A., Harte, J., Hik, D. S., Hofgaard, A., Johnson, D. R., Johnstone, J. F., Jonsdottir, I. S., Jorgenson, J. C., Klanderud, K., Klein, J. A., Koh, S., Kudo, G., Lara, M., Levesque, E., Magnusson, B., May, J. L., Mercado-Diaz, J. A., Michelsen, A., Molau, U., Myers-Smith, I. H., Oberbauer, S. F., Onipchenko, V. G., Rixen, C., Schmidt, N. M., Shaver, G. R., Spasojevic, M. J., Porhallsdottir, P. E., Tolvanen, A., Troxler, T., Tweedie, C. E., Villareal, S., Wahren, C. H., Walker, X., Webber, P. J., Welker, J. M., and Wipf, S.: Plot-scale evidence of tundra vegetation change and links to recent summer warming, *Nat. Clim. Change*, 2, 453–457, doi:10.1038/nclimate1465, 2012.

Fiore, A. M., Naik, V., Spracklen, D. V., Steiner, A., Unger, N., Prather, M., Bergmann, D., Cameron-Smith, P. J., Cionni, I., Collins, W. J., Dalsoren, S., Eyring, V., Folberth, G. A., Ginoux, P., Horowitz, L. W., Josse, B., Lamarque, J.-F., MacKenzie, I. A., Nagashima, T., O'Connor, F. M., Righi, M., Rumbold, S. T., Shindell, D. T., Skeie, R. B., Sudo, K., Szopa, S., Takemura, T., and Zeng, G.: Global air quality and climate, *Chem. Soc. Rev.*, 41, 6663–6683, doi:10.1039/c2cs35095e, 2012.

Fisher, R., McDowell, N., Purves, D., Moorcroft, P., Sitch, S., Cox, P., Huntingford, C., Meir, P., and Woodward, F. I.: Assessing uncertainties in a second-generation dynamic vegetation model caused by ecological scale limitations, *New Phytologist*, 187, 666–681, doi:10.1111/j.1469-8137.2010.03340.x, 2010.

Guenther, A., Hewitt, C. N., Erickson, D., Fall, R., Geron, C., Graedel, T., Harley, P., Klinger, L., Lerdau, M., McKay, W. A., Pierce, T., Scholes, B., Steinbrecher, R., Tallamraju, R., Taylor, J., and Zimmermann, P.: A global model of natural volatile organic compound emissions, *J. Geophys. Res.*, 100, 8873–8892, 1995.

Haapanala, S., Ekberg, A., Hakola, H., Tarvainen, V., Rinne, J., Hellén, H., and Arneth, A.: Mountain birch – potentially large source of sesquiterpenes into high latitude atmosphere, *Biogeosciences*, 6, 2709–2718, doi:10.5194/bg-6-2709-2009, 2009.

Hakola, H., Tarvainen, V., Bäck, J., Ranta, H., Bonn, B., Rinne, J., and Kulmala, M.: Seasonal variation of mono- and sesquiterpene emission rates of Scots pine, *Biogeosciences*, 3, 93–101, doi:10.5194/bg-3-93-2006, 2006.



---

## Future vegetation–climate interactions in Eastern Siberia

A. Arneth et al.

---

Title Page

Abstract

Introduction

Conclusions

References

Tables

Figures

◀

▶

◀

▶

Back

Close

Full Screen / Esc

Printer-friendly Version

Interactive Discussion



Hallquist, M., Wenger, J. C., Baltensperger, U., Rudich, Y., Simpson, D., Claeys, M., Dommen, J., Donahue, N. M., George, C., Goldstein, A. H., Hamilton, J. F., Herrmann, H., Hoffmann, T., Iinuma, Y., Jang, M., Jenkin, M. E., Jimenez, J. L., Kiendler-Scharr, A., Maenhaut, W., McFiggans, G., Mentel, Th. F., Monod, A., Prévôt, A. S. H., Seinfeld, J. H., Surratt, J. D., Szmigielski, R., and Wildt, J.: The formation, properties and impact of secondary organic aerosol: current and emerging issues, *Atmos. Chem. Phys.*, 9, 5155–5236, doi:10.5194/acp-9-5155-2009, 2009.

Hens, K., Novelli, A., Martinez, M., Auld, J., Axinte, R., Bohn, B., Fischer, H., Keronen, P., Kubistin, D., Nölscher, A. C., Oswald, R., Paasonen, P., Petäjä, T., Regelin, E., Sander, R., Sinha, V., Sipilä, M., Taraborrelli, D., Tatum Ernest, C., Williams, J., Lelieveld, J., and Harder, H.: Observation and modelling of HO<sub>x</sub> radicals in a boreal forest, *Atmos. Chem. Phys.*, 14, 8723–8747, doi:10.5194/acp-14-8723-2014, 2014.

Henze, D. and Seinfeld, J. H.: Global secondary organic aerosol from isoprene oxidation, *Geophys. Res. Lett.*, 33, L09812, doi:10.1029/2006GL025976, 2006.

Hickler, T., Vohland, K., Feehan, J., Miller, P. A., Smith, B., Costa, L., Giesecke, T., Fronzek, S., Carter, T. R., Cramer, W., Kuhn, I., and Sykes, M. T.: Projecting the future distribution of European potential natural vegetation zones with a generalized, tree species-based dynamic vegetation model, *Global Ecol. Biogeogr.*, 21, 50–63, doi:10.1111/j.1466-8238.2010.00613.x, 2012.

Holst, T., Arneth, A., Hayward, S., Ekberg, A., Mastepanov, M., Jackowicz-Korczynski, M., Friberg, T., Crill, P. M., and Bäckstrand, K.: BVOC ecosystem flux measurements at a high latitude wetland site, *Atmos. Chem. Phys.*, 10, 1617–1634, doi:10.5194/acp-10-1617-2010, 2010.

Hussein, T., Dal Maso, M., Petäjä, T., Koponen, I. K., Paatero, P., Aalto, P. P., Hämeri, K., and Kulmala, M.: Evaluation of an automatic algorithm for fitting the particle number size distributions, *Boreal Environ. Res.*, 10, 337–355, 2005.

IPCC: Climate Change 2007: The Physical Science Basis, Summary for Policymakers, in: Contribution of Working Group I to the Fourth Assessment Report of the Intergovernmental Panel on Climate Change, Cambridge University Press, Cambridge, 2007.

Jokinen, T., Berndt, T., Makkonen, T., Kerminen, V.-M., Junninen, H., Paasonen, P., Stratmann, F., Herrmann, H., Guenther, A., Worsnop, D. R., Kulmala, M., Ehn, M., and Sipilä, M.: Production of extremely low-volatile organic compounds from biogenic emissions:

## Future vegetation–climate interactions in Eastern Siberia

A. Arneth et al.

[Title Page](#)
[Abstract](#)
[Introduction](#)
[Conclusions](#)
[References](#)
[Tables](#)
[Figures](#)

[Back](#)
[Close](#)
[Full Screen / Esc](#)
[Printer-friendly Version](#)
[Interactive Discussion](#)

Measured yields and atmospheric implications, P. Natl. Acad. Sci. USA, 112, 7123–7128, doi:10.1073/pnas.1423977112, 2015.

Kajos, M. K., Hakola, H., Holst, T., Nieminen, T., Tarvainen, V., Maximov, T., Petäjä, T., Arneth, A., and Rinne, J.: Terpenoid emissions from fully grown East Siberian *Larix cajanderi* trees, Biogeosciences, 10, 4705–4719, doi:10.5194/bg-10-4705-2013, 2013.

Kharuk, V., Ranson, K., and Dvinskaya, M.: Evidence of Evergreen Conifer Invasion into Larch Dominated Forests During Recent Decades in Central Siberia, Euras. J. Forest Res., 10, 163–171, 2007.

Khvorostyanov, D. V., Ciais, P., Krinner, G., and Zimov, S. A.: Vulnerability of east Siberia's frozen carbon stores to future warming, Geophys. Res. Lett., 35, L10703, doi:10.1029/2008GL033639, 2008.

Kobak, K. I., Turchinovich, I. Y., Kondrasheva, N. Y., Schulze, E. D., Schulze, W., Koch, H., and Vygodskaya, N. N.: Vulnerability and adaptation of the larch forest in eastern Siberia to climate change, Water Air Soil Poll., 92, 119–127, 1996.

Koven, C. D., Ringeval, B., Friedlingstein, P., Ciais, P., Cadule, P., Khvorostyanov, D., Krinner, G., and Tarnocai, C.: Permafrost carbon-climate feedbacks accelerate global warming, P. Natl. Acad. Sci. USA, 108, 14769–14774, doi:10.1073/pnas.1103910108, 2011.

Kulmala, M., Dal Maso, M., Makela, J. M., Pirjola, L., Vakeva, M., Aalto, P., Miiikkulainen, P., Hameri, K., and O'Dowd, C. D.: On the formation, growth and composition of nucleation mode particles, Tellus B, 53, 479–490, doi:10.1034/j.1600-0889.2001.530411.x, 2001.

Kulmala, M., Petäjä, T., Mönkkönen, P., Koponen, I. K., Dal Maso, M., Aalto, P. P., Lehtinen, K. E. J., and Kerminen, V.-M.: On the growth of nucleation mode particles: source rates of condensable vapor in polluted and clean environments, Atmos. Chem. Phys., 5, 409–416, doi:10.5194/acp-5-409-2005, 2005.

Lappalainen, H. K., Sevanto, S., Bäck, J., Ruuskanen, T. M., Kolari, P., Taipale, R., Rinne, J., Kulmala, M., and Hari, P.: Day-time concentrations of biogenic volatile organic compounds in a boreal forest canopy and their relation to environmental and biological factors, Atmos. Chem. Phys., 9, 5447–5459, doi:10.5194/acp-9-5447-2009, 2009.

Makkonen, R., Asmi, A., Kerminen, V. M., Boy, M., Arneth, A., Guenther, A., and Kulmala, M.: BVOC-aerosol-climate interactions in the global aerosol-climate model ECHAM5.5-HAM2, Atmos. Chem. Phys., 12, 10077–10096, doi:10.5194/acp-12-10077-2012, 2012a.

## Future vegetation–climate interactions in Eastern Siberia

A. Arneth et al.

Title Page

Abstract

Introduction

Conclusions

References

Tables

Figures

◀

▶

◀

▶

Back

Close

Full Screen / Esc

Printer-friendly Version

Interactive Discussion



- Makkonen, R., Asmi, A., Kerminen, V.-M., Boy, M., Arneth, A., Hari, P., and Kulmala, M.: Air pollution control and decreasing new particle formation lead to strong climate warming, *Atmos. Chem. Phys.*, 12, 1515–1524, doi:10.5194/acp-12-1515-2012, 2012b.
- Miller, P. A. and Smith, B.: Modelling tundra vegetation response to recent arctic warming, *Ambio*, 41, 281–291, doi:10.1007/s13280-012-0306-1, 2012.
- Mitchell, T. D. and Jones, P. D.: An improved method of constructing a database of monthly climate observations and associated high-resolution grids, *Int. J. Climatol.*, 25, 693–712, 2005.
- Moser, L., Fonti, P., Büntgen, U., Esper, J., Luterbacher, J., Franzen, J., and Frank, D.: Timing and duration of European larch growing season along altitudinal gradients in the Swiss Alps, *Tree Physiol.*, 30, 225–233, doi:10.1093/treephys/tpp108, 2012.
- Nieminen, T., Lehtinen, K. E. J., and Kulmala, M.: Sub-10 nm particle growth by vapor condensation – effects of vapor molecule size and particle thermal speed, *Atmos. Chem. Phys.*, 10, 9773–9779, doi:10.5194/acp-10-9773-2010, 2010.
- Niinemets, U., Tenhunen, J. D., Harley, P. C., and Steinbrecher, R.: A model of isoprene emission based on energetic requirements for isoprene synthesis and leaf photosynthetic properties for *Liquidambar* and *Quercus*, *Plant Cell Environ.*, 22, 1319–1335, 1999.
- Niinemets, Ü., Arneth, A., Kuhn, U., Monson, R. K., Peñuelas, J., and Staudt, M.: The emission factor of volatile isoprenoids: stress, acclimation, and developmental responses, *Biogeosciences*, 7, 2203–2223, doi:10.5194/bg-7-2203-2010, 2010.
- O'Donnell, D., Tsigaridis, K., and Feichter, J.: Estimating the direct and indirect effects of secondary organic aerosols using ECHAM5-HAM, *Atmos. Chem. Phys.*, 11, 8635–8659, doi:10.5194/acp-11-8635-2011, 2011.
- Ohta, T., Hiyama, T., Tanaka, H., Kuwada, T., Maximov, T. C., Ohata, T., and Fukushima, Y.: Seasonal variation in the energy and water exchanges above and below a larch forest in eastern Siberia, *Hydrol. Process.*, 15, 1459–1476, 2001.
- Paasonen, P., Asmi, A., Petaja, T., Kajos, M. K., Aijala, M., Junninen, H., Holst, T., Abbatt, J. P. D., Arneth, A., Birmili, W., van der Gon, H. D., Hamed, A., Hoffer, A., Laakso, L., Laaksonen, A., Richard Leaitch, W., Plass-Dulmer, C., Pryor, S. C., Raisanen, P., Swietlicki, E., Wiedensohler, A., Worsnop, D. R., Kerminen, V.-M., and Kulmala, M.: Warming-induced increase in aerosol number concentration likely to moderate climate change, *Nat. Geosci.*, 6, 438–442, doi:10.1038/ngeo1800, 2013.

**Future  
vegetation–climate  
interactions in  
Eastern Siberia**

A. Arneth et al.

Title Page

Abstract

Introduction

Conclusions

References

Tables

Figures



Back

Close

Full Screen / Esc

Printer-friendly Version

Interactive Discussion



- Penuelas, J. and Staudt, M.: Bvocs and global change, *Trends Plant Sci.*, 15, 133–144, doi:10.1016/j.tplants.2009.12.005, 2010.
- Piao, S., Friedlingstein, P., Ciais, P., Zhou, L., and Chen, A.: Effect of climate and CO<sub>2</sub> changes on the greening of the Northern Hemisphere over the past two decades, *Geophys. Res. Lett.*, 33, L23402, doi:10.1029/2006gl028205, 2006.
- Riahi, K., Gruebler, A., and Nakicenovic, N.: Scenarios of long-term socio-economic and environmental development under climate stabilization, *Technol. Forecast. Soc. Change*, 74, 887–935, 2007.
- Rohrer, F. and Berresheim, H.: Strong correlation between levels of tropospheric hydroxyl radicals and solar ultraviolet radiation, *Nature*, 442, 184–187, 2006.
- Romanovsky, V. E., Drozdov, D. S., Oberman, N. G., Malkova, G. V., Kholodov, A. L., Marchenko, S. S., Moskalenko, N. G., Sergeev, D. O., Ukraintseva, N. G., Abramov, A. A., Gilichinsky, D. A., and Vasiliev, A. A.: Thermal state of permafrost in russia, *Permafrost Periglac. Process.*, 21, 136–155, doi:10.1002/ppp.683, 2010.
- Ruuskanen, T. M., Kajos, M. K., Hellén, H., Hakola, H., Tarvainen, V., and Rinne, J.: Volatile organic compound emissions from Siberian larch, *Atmos. Environ.*, 41, 5807–5812, doi:10.1016/j.atmosenv.2007.05.036, 2007.
- Schaefer, K., Lantuit, H., Romanovsky, V. E., Schuur, E. A. G., and Witt, R.: The impact of the permafrost carbon feedback on global climate, *Environ. Res. Lett.*, 9, 085003, doi:10.1088/1748-9326/9/8/085003, 2014.
- Schneider von Deimling, T., Meinshausen, M., Levermann, A., Huber, V., Frieler, K., Lawrence, D. M., and Brovkin, V.: Estimating the near-surface permafrost-carbon feedback on global warming, *Biogeosciences*, 9, 649–665, doi:10.5194/bg-9-649-2012, 2012.
- Schurgers, G., Arneth, A., Holzinger, R., and Goldstein, A. H.: Process-based modelling of biogenic monoterpene emissions combining production and release from storage, *Atmos. Chem. Phys.*, 9, 3409–3423, doi:10.5194/acp-9-3409-2009, 2009a.
- Schurgers, G., Hickler, T., Miller, P. A., and Arneth, A.: European emissions of isoprene and monoterpenes from the Last Glacial Maximum to present, *Biogeosciences*, 6, 2779–2797, doi:10.5194/bg-6-2779-2009, 2009b.
- Schuur, E. A. G., Vogel, J. G., Crummer, K. G., Lee, H., Sickman, J. O., and Osterkamp, T. E.: The effect of permafrost thaw on old carbon release and net carbon exchange from tundra, *Nature*, 459, 556–559, doi:10.1038/nature08031, 2009.

## Future vegetation–climate interactions in Eastern Siberia

A. Arneth et al.

Title Page

Abstract

Introduction

Conclusions

References

Tables

Figures



Back

Close

Full Screen / Esc

Printer-friendly Version

Interactive Discussion



- Serreze, M. C., Walsh, J. E., Chapin, F. S., Osterkamp, T., Dyurgerov, M., Romanovsky, V., Oechel, W. C., Morison, J., Zhang, T., and Barry, R. G.: Observational evidence of recent change in the northern high-latitude environment, *Climatic Change*, 46, 159–207, 2000.
- Shindell, D. T., Levy, H., Schwarzkopf, M. D., Horowitz, L. W., Lamarque, J. F., and Faluvegi, G.: Multimodel projections of climate change from short-lived emissions due to human activities, *J. Geophys. Res.-Atmos.*, 113, D11109, doi:10.1029/2007JD009152, 2008.
- Shuman, J. K., Tchebakova, N. M., Parfenova, E. I., Soja, A. J., Shugart, H. H., Ershov, D., and Holcomb, K.: Forest forecasting with vegetation models across russia, *Can. J. Forest Res.*, 45, 175–184, doi:10.1139/cjfr-2014-0138, 2015.
- Sistla, S. A., Moore, J. C., Simpson, R. T., Gough, L., Shaver, G. R., and Schimel, J. P.: Long-term warming restructures Arctic tundra without changing net soil carbon storage, *Nature*, 497, 615–618, doi:10.1038/nature12129, 2013.
- Sitch, S., Smith, B., Prentice, I. C., Arneth, A., Bondeau, A., Cramer, W., Kaplan, J. O., Levis, S., Lucht, W., Sykes, M. T., Thonicke, K., and Venevsky, S.: Evaluation of ecosystem dynamics, plant geography and terrestrial carbon cycling in the LPJ dynamic global vegetation model, *Global Change Biol.*, 9, 161–185, 2003.
- Sitch, S., Cox, P. M., Collins, W. J., and Huntingford, C.: Indirect radiative forcing of climate change through ozone effects on the land-carbon sink, *Nature*, 448, 791–794, doi:10.1038/nature06059, 2007.
- Smith, B., Prentice, I. C., and Sykes, M. T.: Representation of vegetation dynamics in the modelling of terrestrial ecosystems: comparing two contrasting approaches within European climate space, *Global Ecol. Biogeogr.*, 10, 621–637, 2001.
- Soja, A. J., Tchebakova, N. M., French, N. H. F., Flannigan, M. D., Shugart, H. H., Stocks, B. J., Sukhinin, A. I., Parfenova, E. I., Chapin Iii, F. S., and Stackhouse, J. P. W.: Climate-induced boreal forest change: Predictions versus current observations, *Global Planet. Change*, 56, 274–296, doi:10.1016/j.gloplacha.2006.07.028, 2007.
- Spracklen, D. V., Bonn, B., and Carslaw, K.: Boreal forests, aerosols and the impacts on clouds and climate, *Philos. T. Roy. Soc. Lond. A*, 366, 4613–4626, doi:10.1098/rsta.2008.0201, 2008.
- Spracklen, D. V., Carslaw, K. S., Kulmala, M., Kerminen, V.-M., Sihto, S.-L., Riipinen, I., Merikanto, J., Mann, G. W., Chipperfield, M. P., Wiedensohler, A., Birmili, W., and Lihavainen, H.: Contribution of particle formation to global cloud condensation nuclei concentrations, *Geophys. Res. Lett.*, 35, L06808, doi:10.01029/2007GL033038, 2008b.

## Future vegetation–climate interactions in Eastern Siberia

A. Arneth et al.

Title Page

Abstract

Introduction

Conclusions

References

Tables

Figures



Back

Close

Full Screen / Esc

Printer-friendly Version

Interactive Discussion



Staudt, M., Mandl, N., Joffre, R., and Rambal, S.: Intraspecific variability of monoterpene composition emitted by quercus ilex leaves, *Can. J. Forest Res.*, 31, 174–180, doi:10.1139/x00-153, 2001.

Staudt, M., Joffre, R., and Rambal, S.: How growth conditions affect the capacity of *quercus ilex* leaves to emit monoterpenes, *New Phytologist*, 158, 61–73, 2003.

Stier, P., Feichter, J., Kinne, S., Kloster, S., Vignati, E., Wilson, J., Ganzeveld, L., Tegen, I., Werner, M., Balkanski, Y., Schulz, M., Boucher, O., Minikin, A., and Petzold, A.: The aerosol-climate model ECHAM5-HAM, *Atmos. Chem. Phys.*, 5, 1125–1156, doi:10.5194/acp-5-1125-2005, 2005.

Svenningsson, B., Arneth, A., Hayward, S., Holst, T., Massling, A., Swietlicki, E., Hirsikko, A., Junninen, H., Riipinen, I., Vana, M., dal Maso, M., Hussein, T., and Kulmala, A. E.: Aerosol particle formation events and analysis of high growth rates observed above a sub-arctic wetland–forest mosaic, *Tellus B*, 58, 353–364, doi:10.1111/j.1600-0889.2008.00351.x, 2008.

Takeshi, O., Maximov, T. C., Dolman, A. J., Nakai, T., van der Molen, M. K., Kononov, A. V., Maximov, A. P., Hiyama, T., Iijima, Y., Moors, E. J., Tanaka, H., Toba, T., and Yabuki, H.: Interannual variation of water balance and summer evapotranspiration in an eastern Siberian larch forest over a 7-year period (1998–2006), *Agr. Forest Meteorol.*, 48, 1940–1953, 2008.

Tarnocai, C., Canadell, J. G., Schuur, E. A. G., Kuhry, P., Mazhitova, G., and Zimov, S.: Soil organic carbon pools in the northern circumpolar permafrost region, *Global Biogeochem. Cy.*, 23, Gb2023, doi:10.1029/2008gb003327, 2009.

Tchebakova, N. M., Rehfeldt, G. E., and Parfenova, E. I.: Impacts of climate change on the distribution of *Larix spp.* and *Pinus sylvestris* and their climatypes in Siberia, *Mitig. Adapt. Strat. Global Change*, 11, 861–882, doi:10.1007/s11027-005-9019-0, 2006.

Thonicke, K., Venevsky, S., Sitch, S., and Cramer, W.: The role of fire disturbance for global vegetation dynamics. Coupling fire into a Dynamic Global Vegetation Model, *Global Ecol. Biogeogr.*, 10, 661–678, 2001.

Tsigaridis, K., Daskalakis, N., Kanakidou, M., Adams, P. J., Artaxo, P., Bahadur, R., Balkanski, Y., Bauer, S. E., Bellouin, N., Benedetti, A., Bergman, T., Berntsen, T. K., Beukes, J. P., Bian, H., Carslaw, K. S., Chin, M., Curci, G., Diehl, T., Easter, R. C., Ghan, S. J., Gong, S. L., Hodzic, A., Hoyle, C. R., Iversen, T., Jathar, S., Jimenez, J. L., Kaiser, J. W., Kirkevåg, A., Koch, D., Kokkola, H., Lee, Y. H., Lin, G., Liu, X., Luo, G., Ma, X., Mann, G. W., Mihalopoulos, N., Morcrette, J.-J., Müller, J.-F., Myhre, G., Myriokefalitakis, S., Ng, N. L., O'Donnell,

**Future  
vegetation–climate  
interactions in  
Eastern Siberia**

A. Arneth et al.

Title Page

Abstract

Introduction

Conclusions

References

Tables

Figures



Back

Close

Full Screen / Esc

Printer-friendly Version

Interactive Discussion

D., Penner, J. E., Pozzoli, L., Pringle, K. J., Russell, L. M., Schulz, M., Sciare, J., Seland, Ø., Shindell, D. T., Sillman, S., Skeie, R. B., Spracklen, D., Stavrou, T., Steenrod, S. D., Takemura, T., Tiitta, P., Tilmes, S., Tost, H., van Noije, T., van Zyl, P. G., von Salzen, K., Yu, F., Wang, Z., Wang, Z., Zaveri, R. A., Zhang, H., Zhang, K., Zhang, Q., and Zhang, X.: The AeroCom evaluation and intercomparison of organic aerosol in global models, *Atmos. Chem. Phys.*, 14, 10845–10895, doi:10.5194/acp-14-10845-2014, 2014.

Tunved, P., Hansson, H. C., Kerminen, V. M., Strom, J., Maso, M. D., Lihavainen, H., Viisanen, Y., Aalto, P. P., Komppula, M., and Kulmala, M.: High natural aerosol loading over boreal forests, *Science*, 312, 261–263, doi:10.1126/science.1123052, 2006.

Vignati, E., Wilson, J., and Stier, P.: M7: An efficient size-resolved aerosol microphysics module for large-scale aerosol transport models, *J. Geophys. Res.*, 109, D22202, doi:10.1029/2003JD004485, 2004.

Wagner, V.: Analysis of a Russian landscape map and landscape classification for use in computer-aided forestry research, International Institute for Applied Systems Analysis, Laxenburg, 1997.

Wania, R., Ross, I., and Prentice, I. C.: Integrating peatlands and permafrost into a dynamic global vegetation model: I. Evaluation and sensitivity of physical land surface processes, *Global Biogeochem. Cy.*, 23, GB3014, doi:10.1029/2008GB003412, 2009.

Zaehle, S., Friedlingstein, P., and Friend, A. D.: Terrestrial nitrogen feedbacks may accelerate future climate change, *Geophys. Res. Lett.*, 37, L01401, doi:10.1029/2009GL01345, 2010.

Zhang, K., O'Donnell, D., Kazil, J., Stier, P., Kinne, S., Lohmann, U., Ferrachat, S., Croft, B., Quaas, J., Wan, H., Rast, S., and Feichter, J.: The global aerosol-climate model ECHAM-HAM, version 2: sensitivity to improvements in process representations, *Atmos. Chem. Phys.*, 12, 8911–8949, doi:10.5194/acp-12-8911-2012, 2012.

Zhang, K., Wan, H., Liu, X., Ghan, S. J., Kooperman, G. J., Ma, P.-L., Rasch, P. J., Neubauer, D., and Lohmann, U.: Technical note: On the use of nudging for aerosol–climate model intercomparison studies, *Atmos. Chem. Phys.*, 14, 8631–8645, doi:10.5194/acp-14-8631-2014, 2014.

Zhang, W., Jansson, C., Miller, P. A., Smith, B., and Samuelsson, P.: Biogeophysical feedbacks enhance the arctic terrestrial carbon sink in regional earth system dynamics, *Biogeosciences*, 11, 5503–5519, doi:10.5194/bg-11-5503-2014, 2014.

## Future vegetation–climate interactions in Eastern Siberia

A. Arneth et al.

Title Page

Abstract

Introduction

Conclusions

References

Tables

Figures

◀

▶

◀

▶

Back

Close

Full Screen / Esc

Printer-friendly Version

Interactive Discussion

**Table 1.** Simulated changes in net primary productivity, BVOC emissions, and C pool size in vegetation and soils. Unless stated otherwise, values are for the simulated Siberian domain (76–164° E, 46–71° N), and represent an area of  $1.2E^7$  km<sup>2</sup>.  $NPP_{\text{global}}$  (given as a reference value) is global vegetation net primary productivity. BVOC in Tg C a<sup>-1</sup>, CO<sub>2</sub>-C fluxes in Pg C a<sup>-1</sup>, C pools in PgC. Simulations for monoterpene emissions for the boreal needleleaf summergreen (BNS) plant functional type were made using maximum ( $9.6 \mu\text{g}_C \text{g}^{-1} \text{h}^{-1}$ ) and minimum ( $1.9 \mu\text{g}_C \text{g}^{-1} \text{h}^{-1}$ ) values for  $E^*$  measured in Spasskaya Pad (see text),  $E^* = 6.2 \mu\text{g}_C \text{g}^{-1} \text{h}^{-1}$  represents a weighted average from all observations at the Spasskaya Pad location. For BVOC, CO<sub>2</sub> inhibition was switched on and off (Arneth et al., 2007b).

	1981–2000	2031–2050	2081–2100
$NPP_{\text{global}}$	58 ± 15	66 ± 17	76 ± 14
$NPP$	3.5 ± 0.2	4.5 ± 0.2	5.9 ± 0.2
Carbon in circumpolar permafrost region			
Vegetation	109 ± 0.7	106 ± 1.6	78 ± 1.8
Litter	81 ± 0.5	68 ± 0.3	44 ± 0.3
Soil (0 to 2 m depth)	454 ± 0.03	392 ± 0.4	255 ± 0.5
Total	644 ± 0.4	567 ± 1.1	377 ± 1.0
C-pools in permafrost area of study domain			
Vegetation	41 ± 0.6	38 ± 0.6	35 ± 0.7
Litter	40 ± 0.3	34 ± 0.2	23 ± 0.2
Soil (0 to 2 m depth)	216 ± 0.06	187 ± 0.1	140 ± 0.3
Total	297 ± 0.4	259 ± 0.4	198 ± 0.2
C-pools in entire Siberian study domain			
Vegetation	45 ± 0.5	56 ± 1.5	77 ± 2.8
Litter	41 ± 0.5	43 ± 0.3	41 ± 0.7
Soil (0 to 2 m depth)	219 ± 0.3	221 ± 0.3	223 ± 0.3
Total	305 ± 1.1	320 ± 2.1	342 ± 2.0
BVOC, with CO <sub>2</sub> inhibition			
Total_iso	4.11 ± 0.29	4.52 ± 0.32	4.80 ± 0.24
BNE_MT	1.03 ± 0.07	1.06 ± 0.06	1.02 ± 0.04
BINE_MT	0.23 ± 0.01	0.23 ± 0.01	0.18 ± 0.01
BNS_MT_1.9	0.09 ± 0.01	0.10 ± 0.02	0.09 ± 0.01
BNS_MT_6.2	0.28 ± 0.04	0.33 ± 0.06	0.29 ± 0.04
BNS_MT_9.6	0.43 ± 0.06	0.52 ± 0.09	0.45 ± 0.06
Total_MT <sub>BNS-1.9</sub>	1.40 ± 0.09	1.44 ± 0.10	1.33 ± 0.06
Total_MT <sub>BNS-6.2</sub>	1.60 ± 0.11	1.68 ± 0.14	1.53 ± 0.88
Total_MT <sub>BNS-9.6</sub>	1.75 ± 0.12	1.86 ± 0.16	1.69 ± 0.10
BVOC, no CO <sub>2</sub> inhibition			
Total_iso	3.9 ± 0.29	6.0 ± 0.48	11.0 ± 1.06
BNE_MT	0.99 ± 0.07	1.41 ± 0.1	2.33 ± 0.19
BINE_MT	0.22 ± 0.01	0.30 ± 0.02	0.42 ± 0.02
BNS_MT_1.9	0.08 ± 0.01	0.14 ± 0.02	0.20 ± 0.03
BNS_MT_6.2	0.21 ± 0.03	0.35 ± 0.06	0.52 ± 0.07
BNS_MT_9.6	0.42 ± 0.06	0.69 ± 0.11	1.02 ± 0.13
Total_MT <sub>BNS-1.9</sub>	1.34 ± 0.09	1.92 ± 0.13	3.04 ± 0.23
Total_MT <sub>BNS-6.2</sub>	1.47 ± 0.10	2.13 ± 0.16	3.36 ± 0.27
Total_MT <sub>BNS-9.6</sub>	1.67 ± 0.13	2.47 ± 0.22	4.90 ± 0.47

Abbreviations:  $NPP$ : net primary productivity; BNE: boreal needleleaf evergreen; PFT: shade tolerant; BINE: boreal needleleaf evergreen PFT; intermediate shade-tolerant; BNS: boreal needleleaf summergreen PFT ("tarr"), shade intolerant; continentality index as in Stith et al. (2003); Iso: isoprene; MT: monoterpenes.



## Future vegetation–climate interactions in Eastern Siberia

A. Arneth et al.

Title Page

Abstract

Introduction

Conclusions

References

Tables

Figures

◀

▶

◀

▶

Back

Close

Full Screen / Esc

Printer-friendly Version

Interactive Discussion



**Table 2.** Simulated changes in radiative effects due to change in BVOC emission between years 2000 and 2100, averaged over Siberian domain, Northern Hemisphere and globally. CRF: cloud radiative forcing; CSDRF: direct aerosol effect that accounts only for clear-sky short-wave forcing.

	$\Delta\text{CRF}$ ( $\text{W m}^{-2}$ )	$\Delta\text{CSDRF}$ ( $\text{W m}^{-2}$ )
Siberia	−0.50	−0.21
Northern Hemisphere	−0.30	−0.01
Global	−0.03	−0.01

## Future vegetation–climate interactions in Eastern Siberia

A. Arneth et al.

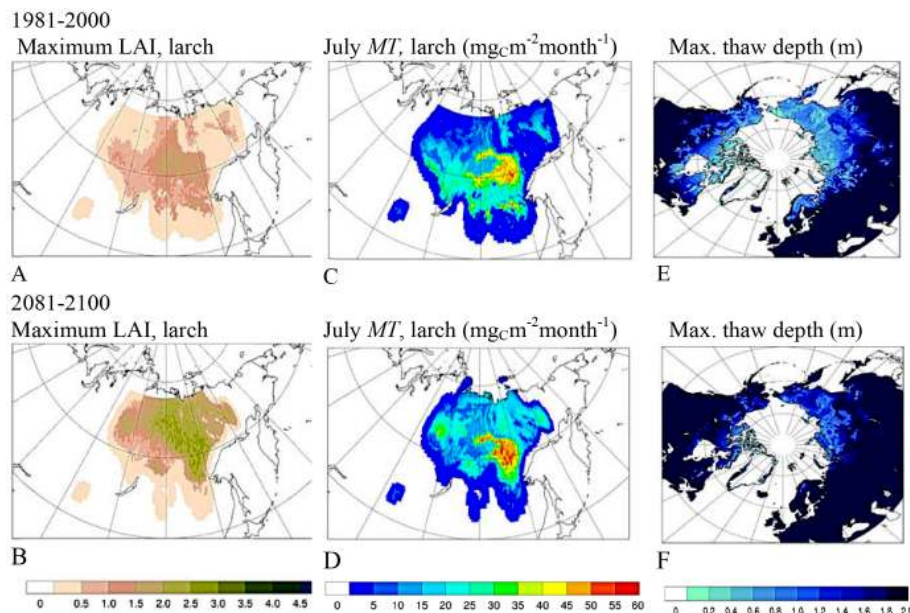


**Figure 1.** Simulated maximum summer leaf area index (LAI; **a**, **b**) and July emissions of monoterpenes (**c**, **d**;  $\text{mg}\cdot\text{C}\cdot\text{m}^{-2}\cdot\text{month}^{-1}$ ) from Eastern Siberian larch. The latter were calculated applying emission factors of 6.2, obtained from the measurements at Spasskaya Pad. (**e**) and (**f**) Maximum permafrost thaw depth (August), shown here as the circumpolar map for comparison with Tarnocai et al. (2009). Values are averages for a simulation 1981–2000 (**a**, **c**, **e**), and for 2081–2100 (**b**, **d**, **f**), applying climate and  $\text{CO}_2$  concentrations from ECHAM-RCP8.5. Emissions in (**c**) and (**d**) do not account for direct  $\text{CO}_2$  inhibition.

## Future vegetation–climate interactions in Eastern Siberia

A. Arneth et al.

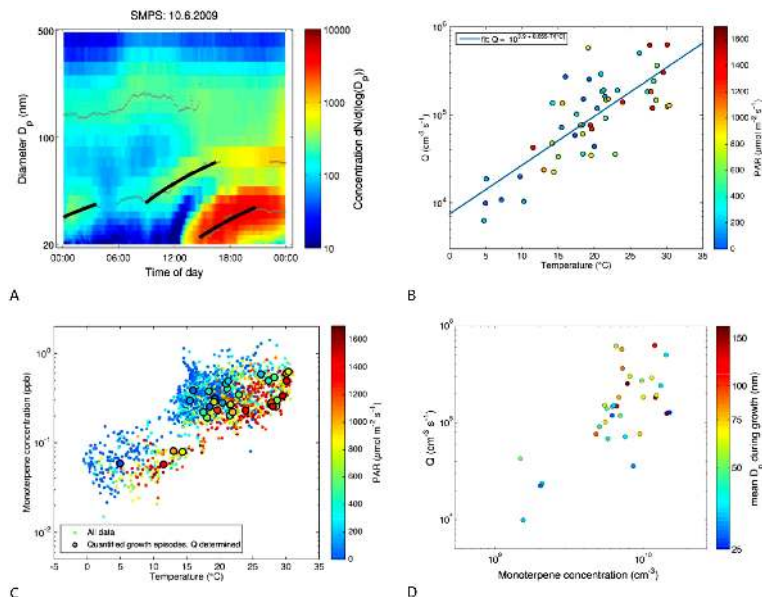


**Figure 2.** Particle growth rates obtained from particle number size distribution (**a**, example from day 10 June 2009). The colours indicate the measured concentrations ( $dN/d\log D_p$ ,  $\text{cm}^{-3}$ ) of particles with different diameters ( $D_p$ , nm) over the course of a day, small circles are mean diameters of concentration modes fitted for each measurement, and the temporal change of these diameters is represented with black lines from which the growth rate is calculated. (**b**) shows the calculated volumetric source rates of condensing vapours ( $Q$ ) as a function of air temperature ( $^{\circ}\text{C}$ ); data are separated by levels of photosynthetically active radiation (PAR). (**c**) Monoterpene concentrations (half hourly data) measured above the canopy vs. temperature measured at the same level (data separated by PAR, the data applied in (**b**) and (**d**) are indicated by encircled symbols), and relationship between volumetric source rate of condensing vapours and monoterpene concentration (**d**; data separated by particle diameter).

## Future vegetation–climate interactions in Eastern Siberia

A. Arneth et al.

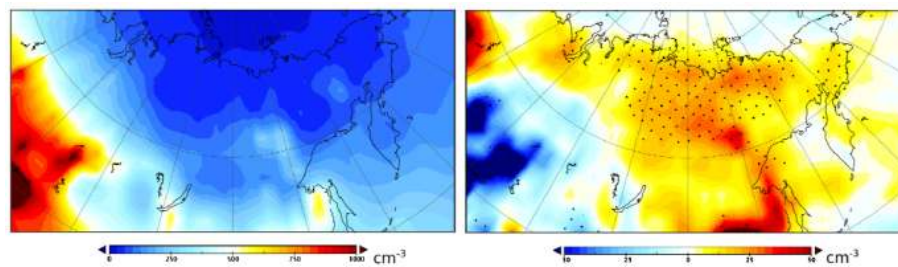


**Figure 3.** Annual average boundary-layer CCN (1.0%) concentration ( $\text{cm}^{-3}$ ) in Siberia with present-day anthropogenic and BVOC (for BNS:  $E^* = 1.9$ ) emissions (left panel), and changes in CCN (1.0%; right panel) concentration due to increase in BVOC emission between years 2000 and 2100 (simulations with  $\text{CO}_2$  inhibition off). Areas with statistical significant changes in CCN are indicated.

[Title Page](#)[Abstract](#)[Introduction](#)[Conclusions](#)[References](#)[Tables](#)[Figures](#)[◀](#)[▶](#)[◀](#)[▶](#)[Back](#)[Close](#)[Full Screen / Esc](#)[Printer-friendly Version](#)[Interactive Discussion](#)

## Future vegetation–climate interactions in Eastern Siberia

A. Arneth et al.

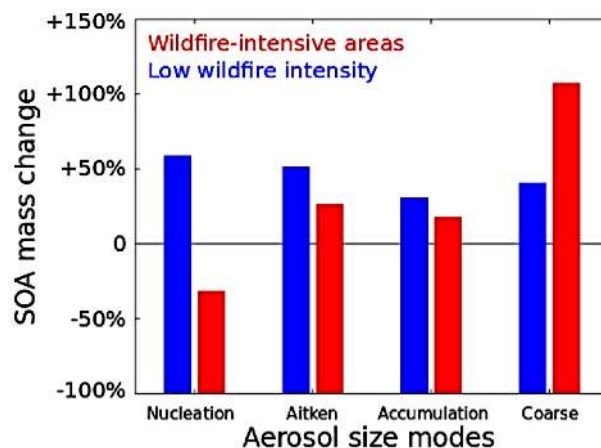


**Figure 4.** Relative increase in SOA mass, simulated by ECHAM5-HAM in different aerosol size modes due to BVOC emissions increase from the year 2000 to 2100. The areas are averaged over Siberia, and the BVOC emissions for years 2000 to 2100 (example is for  $E^* = 1.9$ ). Areas were separated by wildfire emissions (using an emission limit of  $10^{-11} \text{ kg m}^{-2} \text{ s}^{-1}$ ).

[Title Page](#)[Abstract](#)[Introduction](#)[Conclusions](#)[References](#)[Tables](#)[Figures](#)[⏪](#)[⏩](#)[⏴](#)[⏵](#)[Back](#)[Close](#)[Full Screen / Esc](#)[Printer-friendly Version](#)[Interactive Discussion](#)

## Future vegetation–climate interactions in Eastern Siberia

A. Arneth et al.

Title Page

Abstract

Introduction

Conclusions

References

Tables

Figures

◀

▶

◀

▶

Back

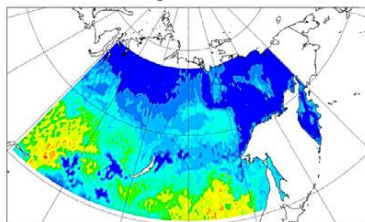
Close

Full Screen / Esc

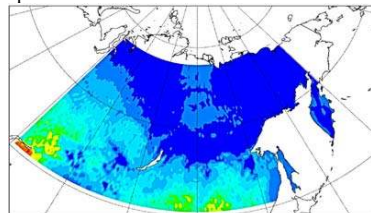
Printer-friendly Version

Interactive Discussion

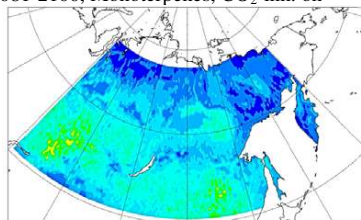
1981–2000, Monoterpenes



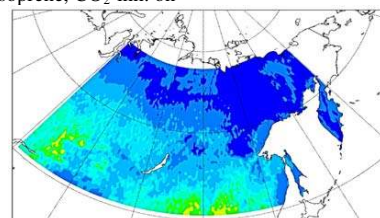
Isoprene



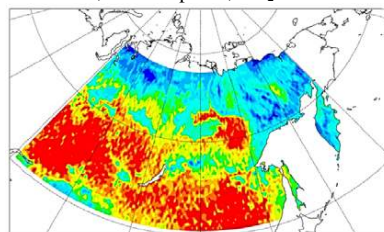
2081–2100, Monoterpenes, CO<sub>2</sub>-inh. on



Isoprene, CO<sub>2</sub>-inh. on



2081–2100, Monoterpenes, CO<sub>2</sub>-inh. off



Isoprene, CO<sub>2</sub>-inh. off

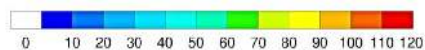
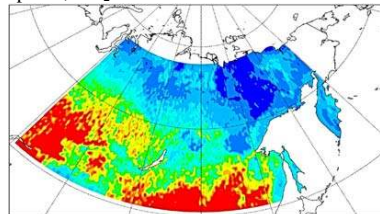


**Figure A1.** Present-day (top panels: 1981–2000) and end of 21st century (bottom panels: 2081–2100) total monoterpene (left panels) and isoprene (right panels) emissions for the month July ( $\text{mg}_C \text{m}^{-2} \text{month}^{-1}$ ). Simulations show results with CO<sub>2</sub> inhibition switched on and off.

## Future vegetation–climate interactions in Eastern Siberia

A. Arneth et al.

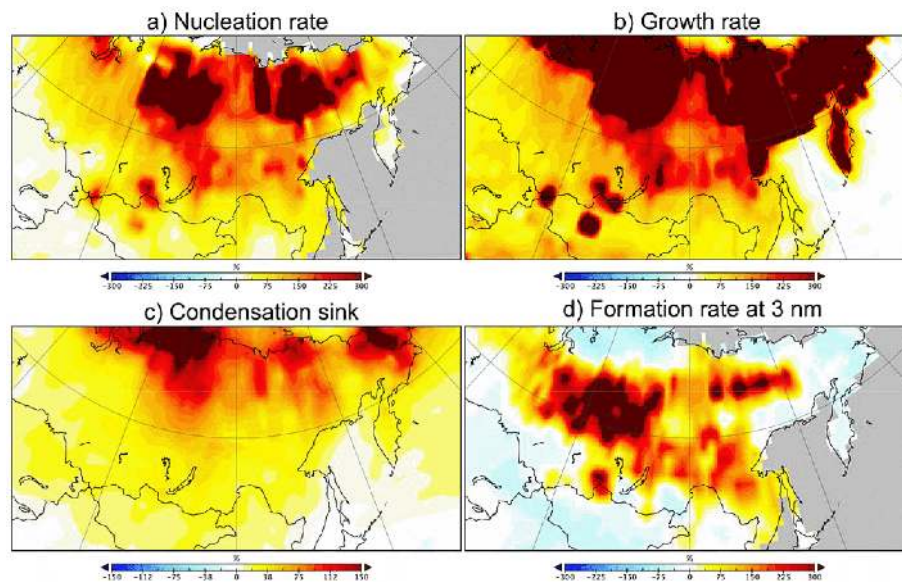


**Figure A2.** Relative change between years 2000 and 2100 (%) nucleation rate **(a)**, growth rate **(b)**, condensation sink **(c)** and formation rate of 3 nm particles in response to altered BVOC emissions (see methods).

Title Page

Abstract

Introduction

Conclusions

References

Tables

Figures

◀

▶

◀

▶

Back

Close

Full Screen / Esc

Printer-friendly Version

Interactive Discussion

